



Formation and phase behavior of porphyrin/arachidic acid mixed systems and morphology study of Langmuir-Schaefer thin films

A J Al-Alwani, V N Mironyuk, M V Pozharov, M V Gavrikov & E G Glukhovskoy

To cite this article: A J Al-Alwani, V N Mironyuk, M V Pozharov, M V Gavrikov & E G Glukhovskoy (2022): Formation and phase behavior of porphyrin/arachidic acid mixed systems and morphology study of Langmuir-Schaefer thin films, *Soft Materials*, DOI: [10.1080/1539445X.2022.2028829](https://doi.org/10.1080/1539445X.2022.2028829)

To link to this article: <https://doi.org/10.1080/1539445X.2022.2028829>



Published online: 20 Jan 2022.



Submit your article to this journal [↗](#)



Article views: 1





View related articles [↗](#)



View Crossmark data [↗](#)



Formation and phase behavior of porphyrin/arachidic acid mixed systems and morphology study of Langmuir-Schaefer thin films

A J Al-Alwani ^a, V N Mironyuk^a, M V Pozharov^b, M V Gavrikov^a, and E G Glukhovskoy ^a

^aEducation and Research Institute of Nanostructures and Biosystems, Saratov State University, Saratov, Russia; ^bInstitute of Chemistry, Saratov State University, Saratov, Russia

ABSTRACT

The paper is focused on the study of the dynamic surface properties of mixed monolayers of porphyrin and arachidic acid with various mole fractions at the air–water interface. The choice of porphyrin solid thin film as an object of study is explained by its high potential application in the area of photovoltaics and medicine. The Langmuir monolayers of porphyrin and arachidic acid were formed under different conditions using the Langmuir-Blodgett technique. The increase of sub-phase temperature led to a decrease in the rigidity of the porphyrin monolayer and leads to accelerating the relaxation process of the monolayer. The chosen surface pressure (4, 5, 15 and 35 mN/m) affected the stability of the floating monolayer. The higher miscibility of the monolayers was obtained at the mole fraction of porphyrin = 0.333. The change in the phase of monolayers surface was reported on the basis of surface potential data. The morphology properties of the mixed systems transferred on silicon substrates by Schaeffer method are studied.

ARTICLE HISTORY

Received 21 September 2021
Accepted 1 January 2022

KEYWORDS

Mixed monolayer; porphyrin; surface pressure; surface potential; compression modulus

Introduction

In the last decade, there has been an active search for molecular systems and technologies for nanoarchitectonics.^[1] This implies a clear control of the chemical composition and structure of functional layers and bulk phases, obtaining a given arrangement of molecules with the required overlap of electrons and the formation of intermolecular bonds, the presence of interlayer correlation of molecules and controlled binding of molecules in adjacent layers, etc. In this regard, there are two main problems to solve, namely – the problem of chemical synthesis of molecular «building» units and the technological problem of developing a method for the formation of structures.

According to many authors, the molecules of porphyrins and their derivatives are rather simple and universal units capable of forming complex molecular ensembles, therefore they are highly useful for nanoarchitectonics. Their primary advantage is the possibility of making small individual variations in the chemical structure of separately selected molecules without disrupting the overall crystal structure of the 2D layer or 3D phase.^[2–4] Porphyrin derivatives have pronounced absorption peaks due to their rich conjugated electron system. They often play the role of effective light-harvesting centers in various molecular systems. This is why they hold great promise for a variety of

applications such as dye-sensitized solar cells, elements of molecular electronics, optically activated chemical nanoreactors, gas sensors, etc.^[5–7]

The overwhelming majority of the ideas of nanoarchitectonics were implemented only “on paper” for only one reason – the lack of proper technology (not only industrial, but also laboratory). There are various methods of formation of thin-film molecularly ordered structures, such as the Langmuir-Blodgett (LB) method,^[8,9] layer-by-layer method,^[10] atomic-layered deposition,^[11] physical vapor deposition,^[12] spin-coating method^[13] and others. Of the above, the Langmuir’s technology provides a unique and simple way to form true monomolecular layers at the air–water interface and to transfer these layers onto a solid substrate in the form of a mono- or multilayer (via several transfer cycles) structure to obtain thin films with high ordering and required properties.^[8,9]

Another nontrivial problem often arises in the case of the formation of monolayers from porphyrin molecules due to the specifics of their intermolecular interactions. Molecules of many porphyrin derivatives tend to form aggregates, thus, making it impossible to obtain a true monomolecular layer. The authors of many studies have tried to control the phase states, parameters and stability of the porphyrin monolayer by varying the external conditions.^[14–16] They tried changing the temperature and acidity of the aqueous subphase, the concentration of

the porphyrin solution, the degree of condensation of molecules on the water surface, etc.; however, no solution to the problem of molecular aggregation has been found.

It is known that complex synergistic effects can be observed in some molecular systems. In this regard, introducing some additives to the main component, porphyrin, can change its intermolecular interactions and reduce molecular aggregation. Of course, in this approach, two extremes can be observed – mutual unlimited dissolution of two components resulting in a completely homogeneous system or phase separation and segregation of one or several components of a mixture.

We chose arachidic acid as an additive for preparing a solution of a mixture of arachidic acid (AA) with porphyrin (**1a**). The structure of AA is close to the structure of substituents in porphyrin molecules, it is a typical surfactant, it forms stable and highly ordered layers, and we have already studied its properties in individual solutions and in compositions with other substances.^[17,18]

Therefore, we would like to present the results of our study of formation of a mixed monolayer of porphyrin and AA with various ratios of initial components. The monolayer was produced via the Langmuir-Blodgett technology that allows the formation of monolayers on the water surface. The correctness of the methods for calculating the parameters of the compression isotherm and their application for the study of new substances was confirmed.

Materials and Methods

Arachidic acid was purchased from Sigma-Aldrich and dissolved in chloroform (Vecton, Russia) producing a 10^{-3} M solution. 5,10,15,20-tetra (4-n-methoxyphenyl)

porphyrin (**1a-16**) was synthesized by Smirnova A.I.,^[19] and dissolved in chloroform producing a 2×10^{-4} M solution. Deionized water produced by Smart2Pure (Thermo Scientific, resistance $18.2 \text{ M}\Omega \times \text{cm}$) was used as a subphase. The chemical structure of the compounds studied is shown in Figure 1. The surface pressure and surface potential isotherms of the formed monolayer were studied using the Langmuir method (KSV NIMA LB Trough Medium KN 2002, Finland) with the KSV NIMA Surface Potential Sensor. The surface potential sensor consists of a probe with a plate that oscillates at a frequency of 140 Hz and an electrode immersed in a subphase. As a result, the method makes it possible to measure the potential difference above and below the layer on the surface of the subphase and is sensitive to the sum of individual dipole moments of molecules at the interface. 100 μl of the mixed solutions were spread on an enclosed subphase surface. The time for evaporation of the solvent from the surface of the subphase was 7 min. The molecules spread at the surface of water were symmetrically compressed by barrier at a speed of 15 mm/min. The isotherms were recorded as a function of monolayers surface area. Atomic force microscopy (AFM) images were taken in semicontact mode by SOLVER Nano AFM microscope. Scanning electron microscopy (SEM) images were taken using a SEM Tescan Mira II LMU microscope (Czech Republic).

Results and Discussion

To determine the parameters of the Langmuir monolayer on the surface of the water subphase, surface pressure and area (π -A) compression isotherms for a various volumes of **1a** and temperature were analyzed. Isothermal dependencies for 100, 150

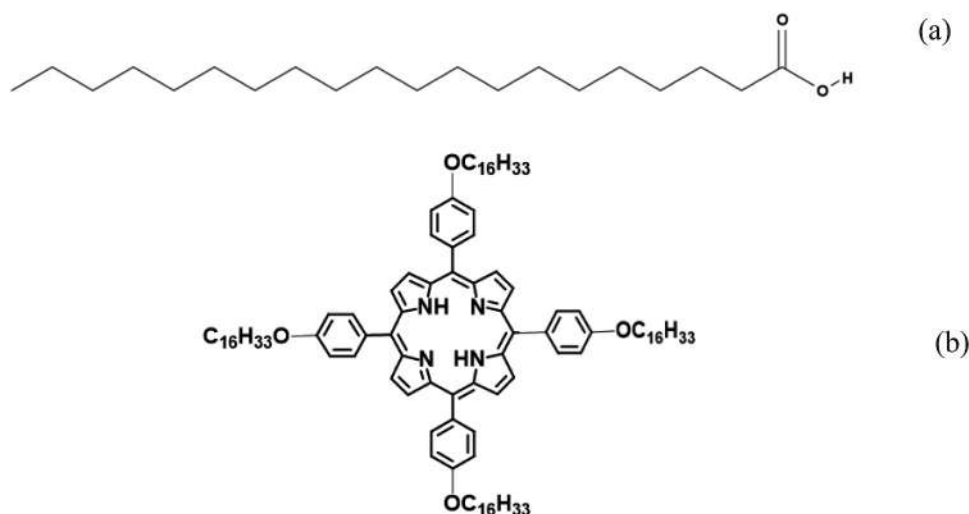


Figure 1. Chemical structures of arachidic acid (a) and Porphyrin (b).

and 200 μl of **1a** are shown in (Fig. 2). In this case, isotherms show the phase transition of **1a** monolayer from gas to solid state. The experimentally obtained monolayer occupied area is comparable with its calculated value (about 75 \AA^2). To describe the processes of formation and destruction of a monolayer, we used the dependences of the surface potential SP [V] on its monolayer area. The surface potential dependences on the π -A isotherms recorded during compression made it possible to study the observed phase transformations at the early stages of the compression in greater detail (Fig. 2). When the monolayer was compressed, a sharp jump in the surface potential was observed corresponding to the onset of monolayer formation over the area of 100 \AA^2 , which is in agreement with Langmuir isotherm at volume 100 μl . The surface potential result showed that the minimum value at 170 \AA^2 , and then the isotherm started rising due to the change in the orientation of porphyrin with respect to the water surface. This result suggests the position of porphyrin oriented perpendicularly to the surface of the water subphase, in accordance with the literature data.^[14] The surface pressure of **1a** did not show the significant changes indicating of the monolayer collapse. For area greater than 85 \AA^2 the system exist in a gas phase; the area range of 69 to 85 \AA^2 corresponds to formation of a monolayer of porphyrin at the water interface leading to orientation of porphyrin molecules with hydrophobic hexadecyloxygroups (having a small negative charge) oriented toward the air, thus contributing to

negative surface charge. Further condensation (below 69 \AA^2) results in formation of a bilayer (according to Volmer method^[20,21]) of porphyrin and arachidic acid molecules; this bilayer has a positive surface charge due to accumulation of protons from the acid on nitrogen atoms of porphyrin molecules resulting from their interaction.

During the experiments, we obtained a series of isotherms for each solution and various temperatures of the subphase. The effect of temperature on the π -A isotherms of **1a** monolayer at higher volume (200 μL) and speed of barrier movement (15 mm/min) at fixed temperatures of 19, 24, 33 and 41°C (the margin of error for thermal stabilization of the process is 0.1°C) were investigated. For higher subphase temperatures, there is a notable shift of the π -A isotherms to the left corresponding to a reduction of the **1a** monolayer area. Compression of the monolayer by symmetrical movable barriers leads to an initial increase of surface pressure, the higher value of surface pressure showed 27.59 mN/m at a subphase temperature of 19°C caused by an increase in the dynamic elasticity of the monolayer. The increase of subphase temperature from 19 to 24°C leads to a decrease in the surface pressure of **1a** monolayer by up to 45%, while, at 41°C the surface pressure decreased by 89%. The correlation of compression modulus of **1a** monolayer with its surface pressure at various temperatures is shown in (Fig. 3). Obviously, the value of rigidity decreases linearly as the temperature of subphase increases. Further compression of the **1a** monolayer did not lead to the expected collapse at the selected volume, that can be

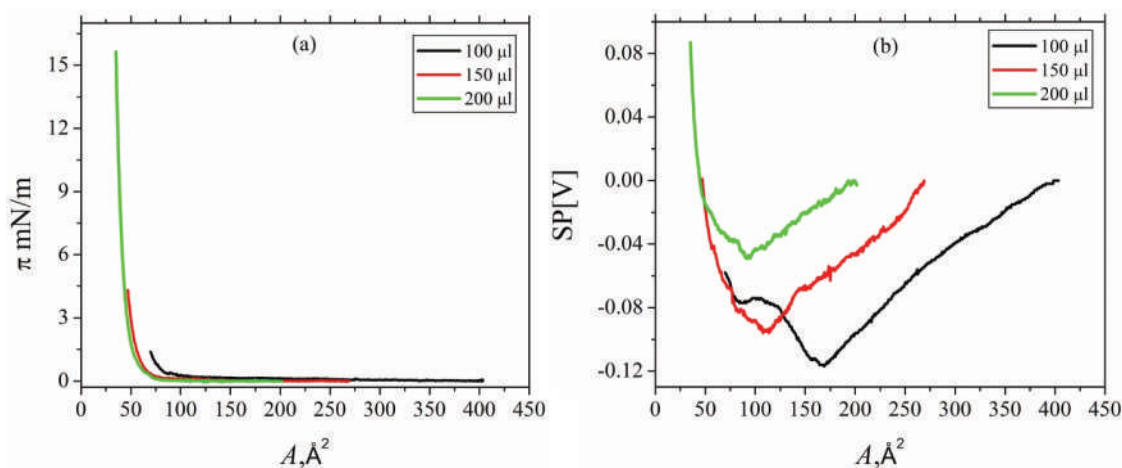


Figure 2. LB isotherm (a) and surface potential (b) of **1a** monolayer at different volume ratio.

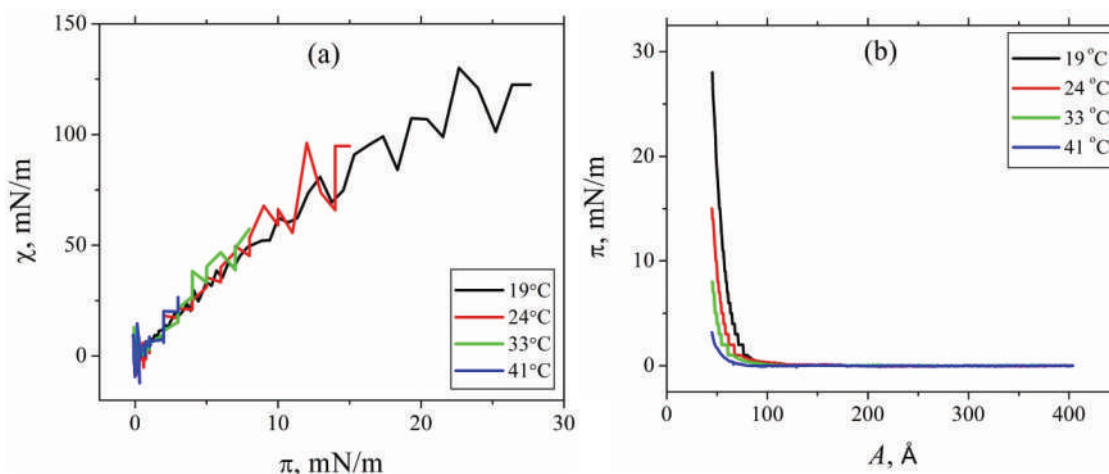


Figure 3. Compression modulus (a) and surface pressure isotherms per area (b) of **1a** Langmuir monolayers at different temperatures.

probably explained by expulsion of **1a** molecules from the monolayer at the water surface into the inner layers of the subphase. The data analysis of the compression and expanding isotherms also indicate of the destruction of the monolayer as it stretches during the reverse stroke of the barriers.

The behavior of the $(dA/d\pi)$ derivative is inversely proportionate with the behavior of the parameter of the modulus of compressibility χ ^[22,23] calculated by the formula (1):

$$\chi = \frac{1}{K}, K = -\frac{1}{A} \left(\frac{dA}{d\pi} \right) \quad (1)$$

where dA is the change in the monolayer area, $d\pi$ is the change in the value of the surface pressure, A is the area occupied by the monolayer in the close-packed state. The results demonstrate that by increasing the subphase temperature, the χ value decreases by 13.46 and 18.95% at 33 and 41°C, respectively, i.e. the stiffness increased (Fig. 3). The modulus of compression of the monolayer film corresponded to the liquid phase.^[24]

The **AA** monolayer hysteresis was investigated (SI Figure S1), 50 μ l of the worked solution was spread on the surface of subphase. The arrows with isotherms show the compression and decompression of three cycles. According to our study, compression and decompression cycles reduce the area of isotherm with increase in the number of cycles. The area settles into a reduced value from 34 \AA^2 , to 32 and 25 \AA^2 , after the second and third compression, that indicates of the change in the stability of the **AA** monolayer; however, the surface pressure has not been reduced. The isotherm of the first cycle of **AA** monolayer area shows that at the 28

\AA^2 , the surface pressure formed up from 26 mN/m and rises steeply to 52.5 mN/m. The compression and expansion isotherms of the monolayers were investigated at 24°C. The results show that the transition between liquid expanded and liquid condensed phases is reversible, however, the value of surface pressure and occupied area have been reduced due to the change in the dynamic surface properties of the Langmuir monolayer.

The influence of barrier speed on the properties of **AA** isotherm has been investigated (SI Figure S2), it was shown that when barrier speed increases from 15 to 40 mm/min, the occupied area is reduced by 2.3%, however, when the speed changes to 1 mm/min, the occupied area is increased by 1.2%. The value of the specific area per molecule for arachidic acid in the region of high pressures is in the range of ($\sim 0.23 \text{ nm}^2$). This value highly correlates with the results obtained earlier.^[25] The influence of the surface pressure on the stability of **AA** Monolayer was considered (SI Figure S3). We found the chosen surface pressure values (4, 5, 15 mN/m) have the same effect on the relaxation area of monolayer reduced by 0.4% over time. However, the monolayer area was reduced by 7.15% over time at fixed surface pressure of 35 mN/m.

Figure 4 shows the isotherms of mixtures of **1a** and **AA** as a function of mole fraction ($X_{1a} = 0.333, 0.285, 0.230, 0.091, 0.047, 0.032, 0.006, 0.003, \text{ and } 0$). Further increase in the of mole fraction of **1a** leads to negligible changes. According to Figure 4, we can see that a notable increase in the number of arachidic acid molecules in the working mixture decreases the length of the gas phase of the monolayer. This can attributed to the fact that increase in the number of arachidic acid molecules leads to an increase in the amount of the component of the solution area on the surface of the aqueous subphase, leading to an

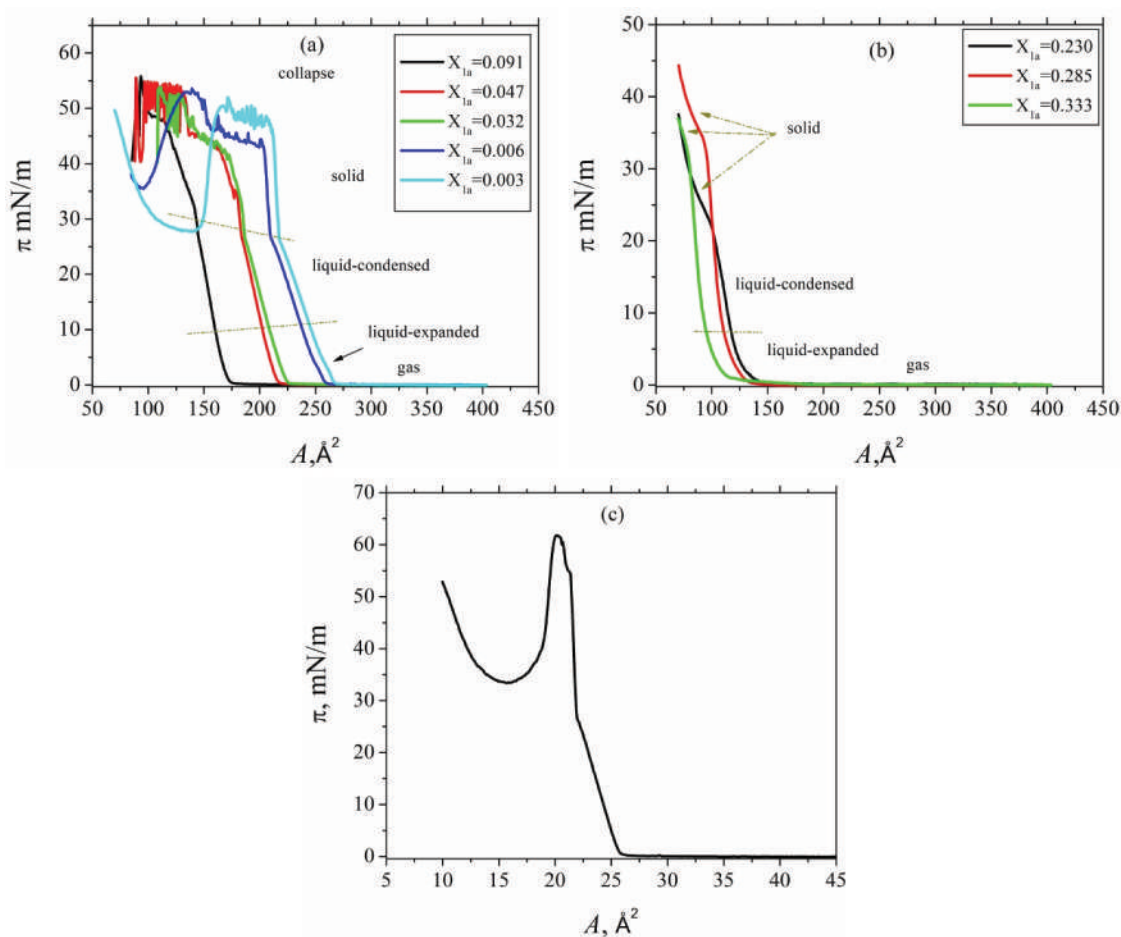


Figure 4. Surface pressure isotherms for the mixed monolayer of **AA** in a molar fraction X of **1a** (a) and (b), and isotherm for pure **AA** (c).

increase in surface pressure and eventual collapse of the monolayer. The values of the limiting Langmuir area (condensed phases) decrease with decreasing molar

fraction of **AA**. Thus, at a mole fraction ($X_{1a} = 0.003$), the **1a** and **AA** isotherm turns into a maximal condensed monolayer as the occupied area of layer decreases.

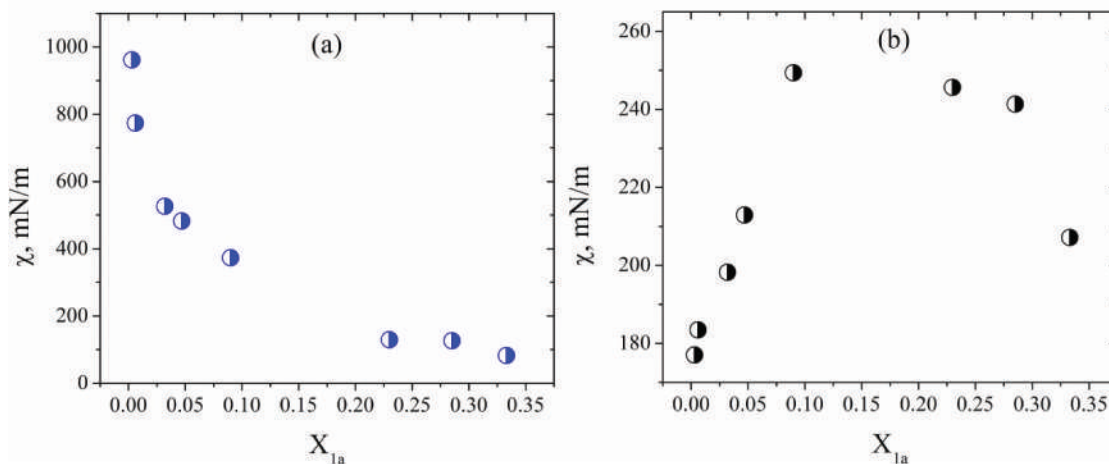


Figure 5. Compression modulus χ of (solid phase, Figure 4) (a) and (liquid-condensed phase, Figure 4) (b) of **1a:AA** monolayers as a function of mole fraction.

The values of the surface potential show a sharp increase at a given critical area for ($X_{1a} = 0.091$ and 0.230). This behavior can be attributed to the structuring of the monolayer that causes the effective dielectric constant at the film-water interface to increase drastically (SI Figure S4). The collapse pressure increases with decreasing the mole fraction of **1a** from (0.091 to 0.006), with collapse described by a change in isotherm slope as the surface pressure rises.

The differences in mechanical properties (compressibility modulus) of liquid-condensed and solid phases of mixed monolayers have been investigated (Fig. 5). In this regard, the search for the ranges with the steepest slope of the isotherm can be performed directly from the graph of the dependence of χ on area (formula, 1).

Figure 5 shows simultaneous χ dependences for mixed monolayer of **AA** in a molar fraction X of **1a**. The minimum value of the modulus of compression at $X_{1a} = 0.333$ corresponds to the liquid phase of the monolayer (liquid-expanded/liquid-condensed phase (LE/LC)) (Fig. 5a). However, the higher value compression modulus showed at $X_{1a} = 0.003$ can be attributed to condensed phase (C).^[26,27] The value of χ exhibits polynomial growth.

In Figure 5b, a distinctive feature of this isotherm is the presence of several areas where the restructuring of the monolayer structure took place. The higher compressibility modulus χ value showed at $X_{1a} = 0.091$ corresponds to LE/LC phase with the minimal χ value is observed for $X_{1a} = 0.003$.

The interactions between molecules in monolayers of mixtures were quantified by calculating excess area (A_E). A_E can be calculated quantitatively by analyzing the isotherms of individual components and their binary mixtures:

$$A_E = A_{12} - (X_1A_1 + X_2A_2), A_{id}=X_1A_1 + X_2A_2$$

where A_1 and A_2 are the average molecular areas of the **1a** and **AA** components, respectively, A_{12} is the average molecular area of the mixture monolayer, and X_1 and X_2 are the mole fractions of the mixture components, A_{id} is the ideal mean monolayers area. According to,^[28] if the value of A_E is zero, it means that the mixed monolayer is perfectly mixed. If the A_E deviate to the negative or positive values, this means the mixed monolayer has less miscibility. The mole fraction of **1a** (0.230) showed the highest value of excess area, however the mole fraction of **1a** at 0.003 showed the minimum value and the highest stability in comparison with other ratios (Fig. 6) that is comparable to results shown in.^[29] The value excess area is not equal to zero means that the miscibility of the mixed monolayer has different mechanisms and repulsive interaction between the mixed molecules. The surface potential data showed that the miscibility is not only dependent on the mole fraction but also on the direction or the orientation by molecules.

On (Fig. 7), the black solid dots show the area of the mixed monolayers at effective states. The straight blue solid line represents the ideal mixed monolayers with the theoretical area. We can emphasize that molar fraction of **1a** has an important influence on the interactions between **1a** and **AA** molecules. Figure 7 shows that the mean monolayer area of

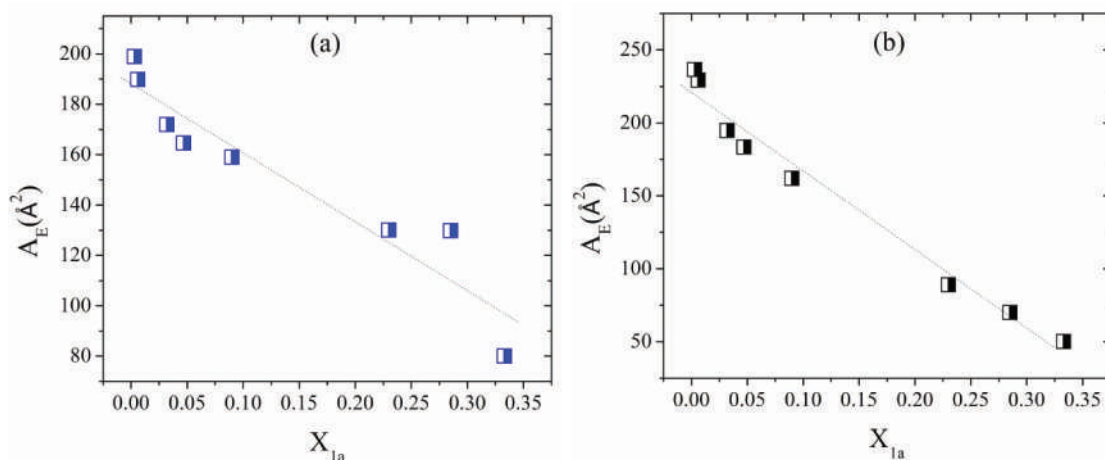


Figure 6. The excess area A_E as a function of mole fractions of **1a:AA** monolayers for solid phase (a), liquid-condensed phase (b).

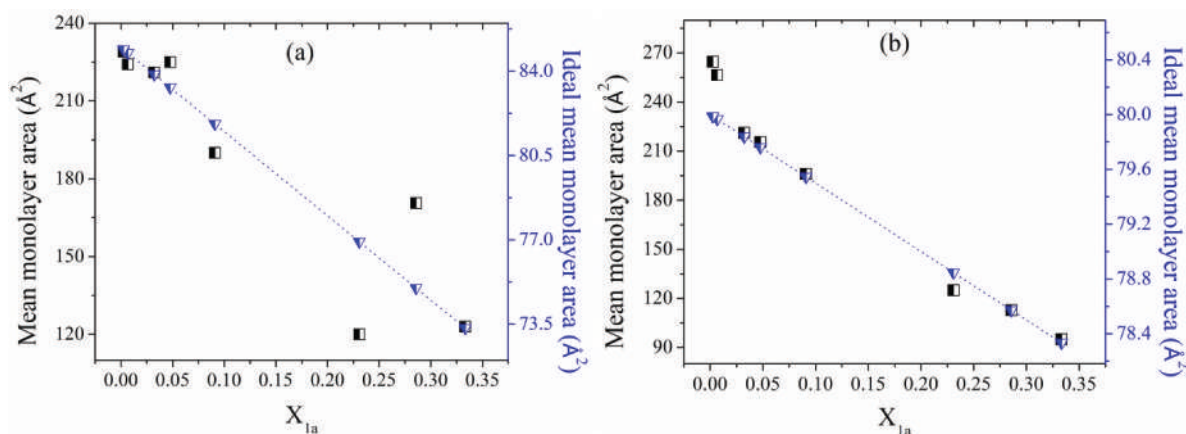


Figure 7. Mean molecular area as a function of the mole fraction of **1a** in the mixed with **AA** on water subphase, solid phase (a) and liquid-condensed phase (b).

mixture decreases with the increment of mole fraction of **1a**. The mean monolayer areas of Langmuir monolayer as a function of the mole fraction of **1a** (0.333, 0.285, 0.230, 0.091, 0.047, 0.032, 0.006, and 0.003) is shown in (Fig. 7). Relaxation data indicates that the dissolution of the mixed monolayer is suppressed by **1a**. The most stable mixed monolayers are formed at a mole fraction of **1a** is 0.003, in agreement with the calculated excess area. Thus, we can see that the curves of the mean monolayer area exhibits nonlinear characteristics for different mole fractions. It suggests that **1a** and **AA** monolayers are interacting at subphase surface and may be miscible at the air–water interface. We also found that the experimental curves were almost in agreement with the theoretical ones at 0.285, 0.333, 0.091, 0.047, and 0.032 mole fractions for (liquid-condensed phase, Figure 4), and 0.333, 0.032, 0.006, and 0.003 mole fractions of **1a** for (solid phase, Figure 4).

Typical AFM images for films on solid substrates are shown in (Fig. 8). According to (Fig. 8), the surface of the substrates is almost completely covered with a monolayer. The monolayer with mole fraction of **1a** at 0.333 shows the highest average roughness value (7.95 nm) at surface pressure of 20 mN/m, however the highest value of 8.68 nm is registered for monolayer with $X_{1a} = 0.091$ at surface pressure of 31 mN/m (Fig. 9). The highest thickness (21.24 nm) is observed by increasing mole fractions 0.003 of **1a** at surface pressure of 31 mN/m. The obtained thin films have a more homogeneous surface at surface pressure of 20 mN/m, the increase of surface pressure leads to disorder of mixed monolayer structure at air–water interface.

The structure of **1a:AA** monolayers at the air–water interface may change at a surface pressure of about 31 mN/m resulting in a decrease of the occupied area by 59 \AA^2 . In this case, the change in the structure of monolayer will be caused either by a shift in the orientation of the porphyrin rings or by the extrusion of mixed monolayers as suggested by results obtained at surface pressures of about 31 mN/m or higher.

Thus, during our study, we were able to establish that an increase in the mole fractions of **AA** in a solution with **1a** makes it possible to achieve the formation of higher stability monolayer and more homogeneous thin film. Experiments have also shown that the best technique for transferring the hydrophobic part of **1a:AA** monolayers to solid substrates (silicon substrate coated with SiO_2 about 40 \AA) by Schaeffer method (with a direction from upper surface of water).

The relaxation time of monolayers occupied area at different mole fractions was considered. The monolayers of **1a:AA** were compressed with the rate of 15 mm/min at surface pressure value of 5 mN/m, at subphase temperature of 25°C. The results showed that the occupied area has decreased to 87, 5, 1, and 0.3% of initial area at $X_{1a} = 0.333, 0.230, 0.091, 0.047$, and 0.032, respectively. However, there is an increase in the relaxation time of occupied area to 0.19 and 0.23% at $X_{1a} = 0.003$ and 0.006, respectively. The experimental results of ($X_{1a} = 0.091, 0.047$ and 0.032, 0.285 and 0.333) were approximated by exponential relationship^[30] (SI Figure S5).

Changes in surface potential of mixed monolayer over time (approximately 2135 seconds) are shown in (SI Figure S6). The results show that the surface potential values of mixed monolayer were drifting linearly over time, with the drift average values over time being

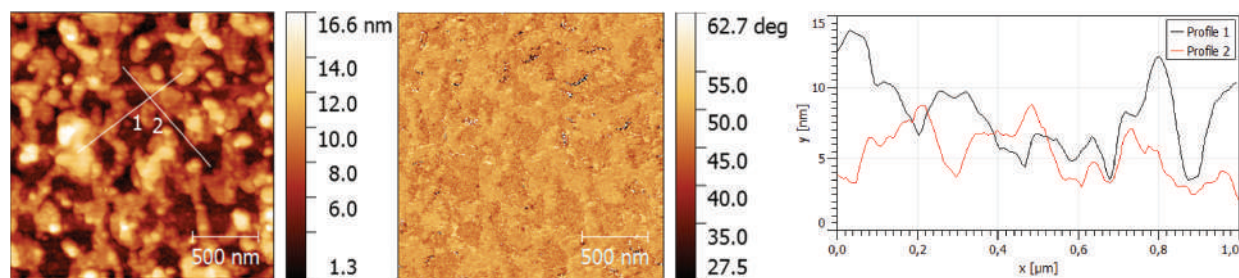
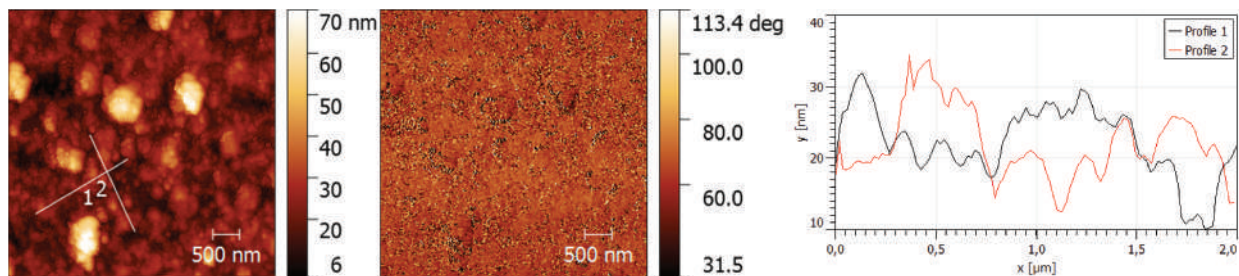
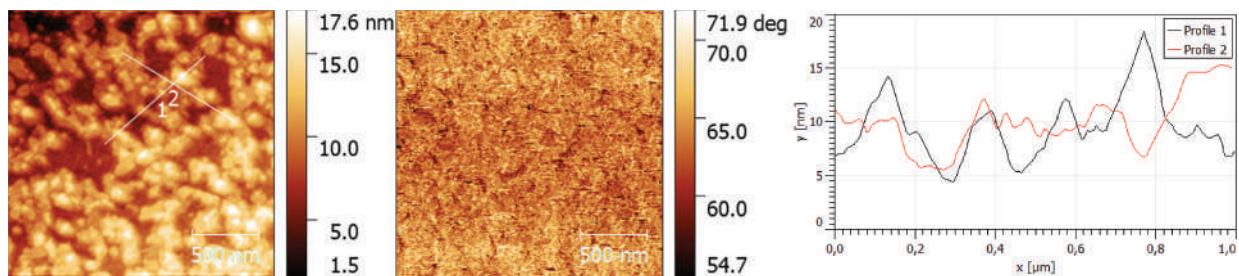
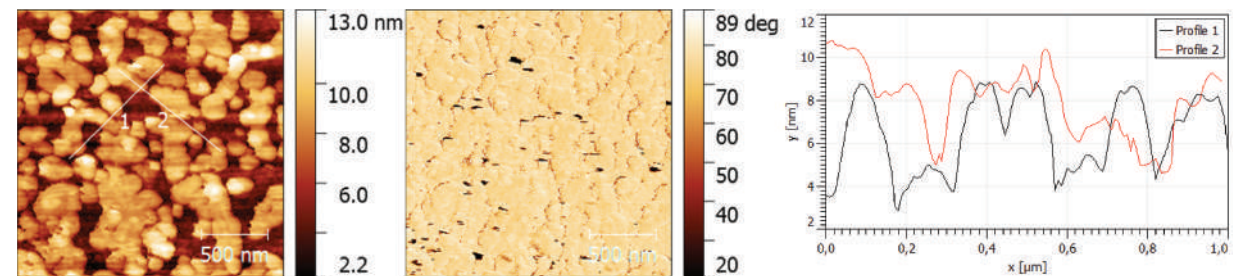
(a) **1a:AA**, $X_{1a}=0.091$ at 20mN/m(b) **1a:AA**, $X_{1a}=0.091$ at 31mN/m(c) **1a:AA**, $X_{1a}=0.230$ at 20mN/m(c) **1a:AA**, $X_{1a}=0.230$ at 31mN/m

Figure 8. AFM, phase and profile images of films of the **1a:AA** mixture as a function of the mole fraction and surface pressure. (a) **1a:AA**, $X_{1a} = 0.091$ at 20mN/m (b) **1a:AA**, $X_{1a} = 0.091$ at 31mN/m (c) **1a:AA**, $X_{1a} = 0.230$ at 20mN/m (c) **1a:AA**, $X_{1a} = 0.230$ at 31mN/m (d) **1a:AA**, $X_{1a} = 0.003$ at 20mN/m (e) **1a:AA**, $X_{1a} = 0.003$ at 31mN/m (f) **1a:AA**, $X_{1a} = 0.333$ at 20mN/m (g) **1a:AA**, $X_{1a} = 0.333$ at 31mN/m

0.007 and 0.033 V for $X_{1a} = 0.091$ and 0.230, respectively. The surface potential of mixed monolayer as a function of the mole fraction of **1a** was shown in (Fig. 10). The highest value of SP [V] is observed at 0.091 mole fraction of **1a**. The higher is the value of mole fraction of **1a** (0.333) the lower is the surface

potential. During compression of Langmuir monolayer, the hydrophobic part of the molecule begins to stretch out at the surface of the subphase and the dipole moment causes an increase of the surface potential value that corresponds to the lifting point of the Langmuir surface pressure.

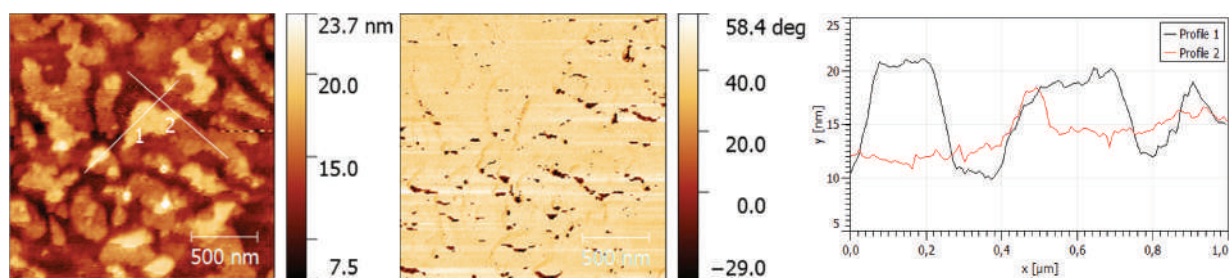
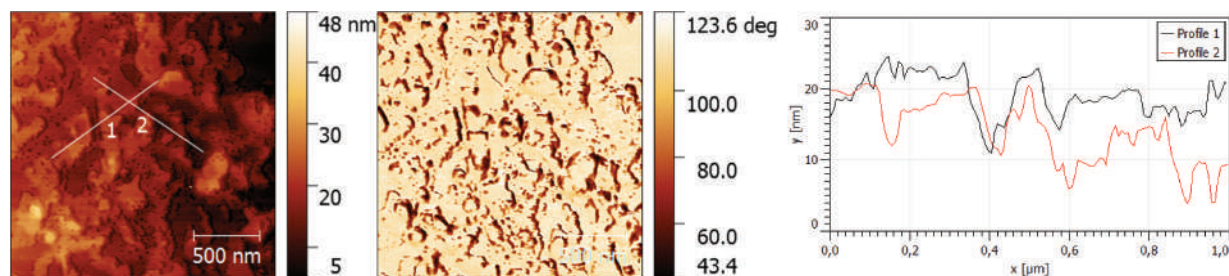
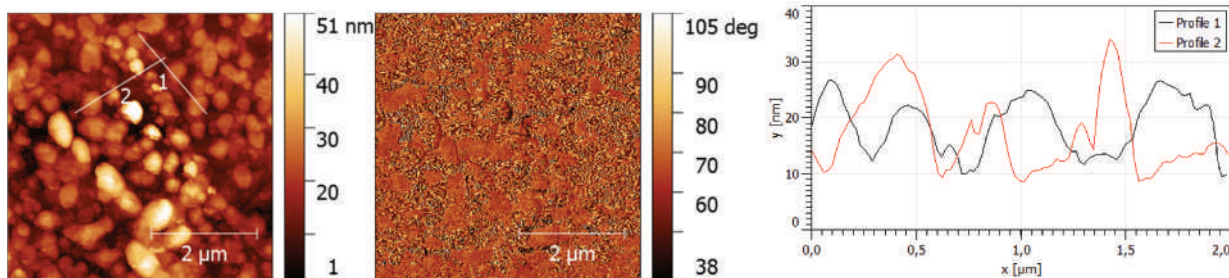
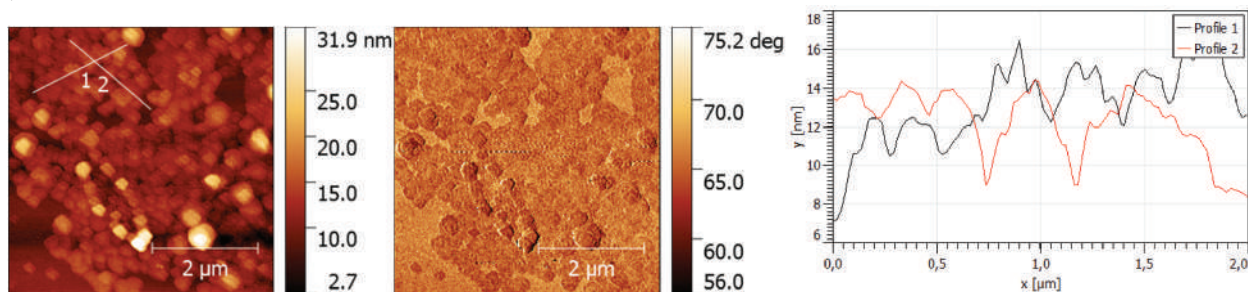
(d) **1a:AA**, $X_{1a}=0.003$ at 20mN/m(e) **1a:AA**, $X_{1a}=0.003$ at 31mN/m(f) **1a:AA**, $X_{1a}=0.333$ at 20mN/m(g) **1a:AA**, $X_{1a}=0.333$ at 31mN/m

Figure 8. Continued.

The change of surface potential (ΔV) value correlates with the interfacial change of the dipole density

$$\Delta V = \frac{\mu_{\perp}}{A \epsilon_r \epsilon_0}$$

where μ_{\perp} is the effective dipole moment, A is the area on the surface of the subphase occupied by the monolayer, ϵ_r and ϵ_0 are the values of the dielectric constant of the monolayer and vacuum, respectively ($\epsilon_0 = 8.85 \times 10^{-12}$ F/m).^[31,32] The dipole moment value is positive when molecule is directed from the water surface (negative) toward the air (positive).

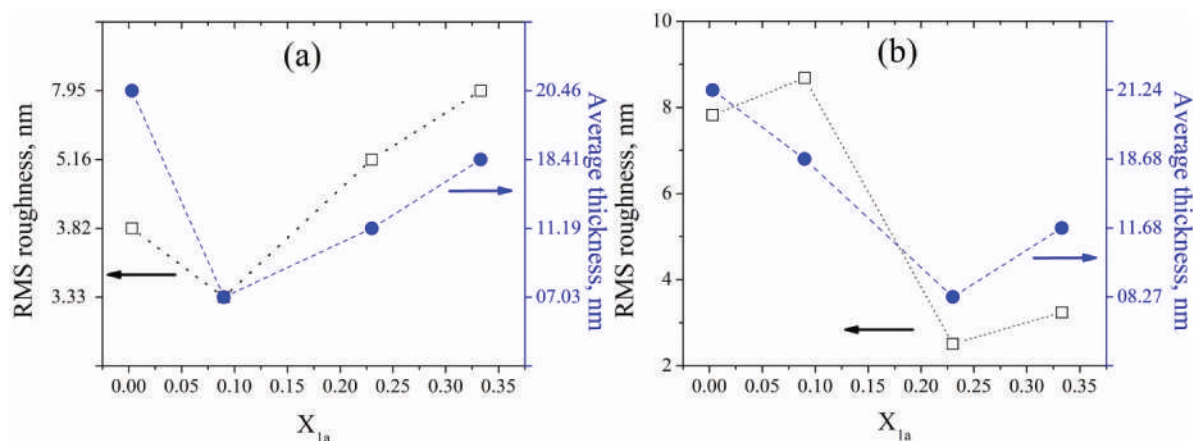


Figure 9. Roughness value (RMS) and average thickness of **1a:AA** as a function of the mole fraction at surface pressure of 20 mN/m (a) and 31 mN/m (b).

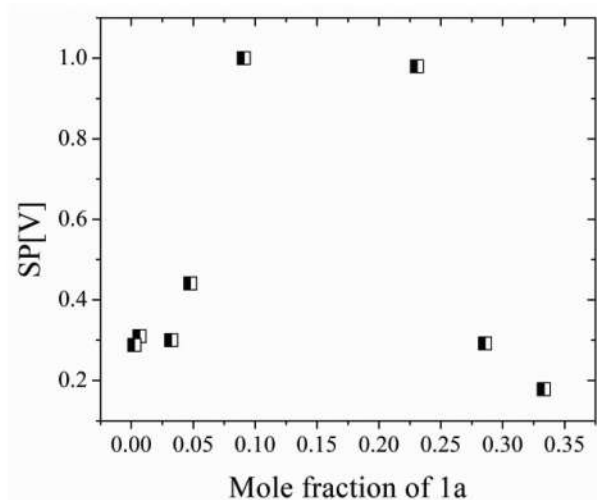


Figure 10. Surface potential as a function of the mole fraction of **1a** in the mixed with **AA** on the water subphase.

Conclusion

The surface properties of **1a:AA** mixed monolayers were studied at different mole fractions. The interaction between **1a** and **AA** monolayer has been investigated by analyzing the excess monolayer area, the dynamic stability, and the morphology properties of the thin films. The result showed that the presence of the **AA** molecules with **1a** lead to the formation of a stable Langmuir film at the air-water interface. The higher miscibility of mixed monolayer was obtained at $X_{1a} = 0.333$. The data was studied with compression/expansion methods and by studying the stability of the monolayer over time. The mole fractions of studied solution spread over the subphase surface is specified from the principle properties of Langmuir monolayer (occupied area, and change in the phase of the registered isotherms). According to our study, the formation of the

AA Langmuir monolayer was reversible, suggesting the self-assembly or domain formation of **AA** monolayer. We found that the increase of subphase temperature leads to a decrease in the rigidity of **1a** monolayer due to the dissolution and disruption of the monolayer structure. Occupied area relaxation and surface rigidity measurements at different mole fraction showed the slowing of the relaxation in mixed monolayers with the increase the mole fraction of **AA**. One of the main purposes is to establish the required conditions for the formation and deposition of a mixed monolayer of **1a** and **AA** for further applications in dye-sensitized solar cells. The higher mole fraction of **AA** is the more optimal ratio of the **1a:AA** mixture. The surface compressibility value of the mixed Langmuir monolayers improved with the presence of **AA** molecules. It was found that the AFM images of mixed monolayers are dependent on the **1a** mole fraction and deposition surface pressure. The proposed method for the formation of composite films with **1a** in their composition is a new approach to obtaining ordered structures with **1a** and **AA**.

Acknowledgments

This work is supported by a grant from the Russian Science Foundation (project No. 21-73-20057) and Saratov State University.

Disclosure statement

The authors report no declarations of interest.

Funding

This work was supported by the Russian Science Foundation [21-73-20057].

ORCID

A J Al-Alwani  <http://orcid.org/0000-0002-5665-464X>
 E G Glukhovskoy  <http://orcid.org/0000-0002-8282-3638>

References

- [1] Ariga, K.; Jia, X.; Song, J.; Hill, J. P.; Leong, D. T.; Jia, Y.; Li, J. Nanoarchitectonics beyond Self-Assembly: Challenges to Create Bio-like Hierarchic Organization. *Angew. Chem. Int. Ed.* **2020**, *59*(36), 15424–15446. DOI: [10.1002/anie.202000802](https://doi.org/10.1002/anie.202000802).
- [2] Beuerle, F.; Gole, B. Covalent Organic Frameworks and Cage Compounds: Design and Applications of Polymeric and Discrete Organic Scaffolds. *Angew. Chem. Int. Ed.* **2018**, *57*(18), 4850–4878. DOI: [10.1002/anie.201710190](https://doi.org/10.1002/anie.201710190).
- [3] Silva, J. D. A. E.; Domingos, V. F.; Marto, D.; Costa, L. D.; Marcos, M.; Silva, M. R.; Gil, J. M.; Sobral, A. J. F. N. Reversible Sequestering of CO₂ on a Multiporous Crystalline Framework of 2-Quinoly-porphyrin. *Tetrahedron Lett.* **2013**, *54*(20), 2449–2451. DOI: [10.1016/j.tetlet.2013.02.071](https://doi.org/10.1016/j.tetlet.2013.02.071).
- [4] Huang, N.; Krishna, R.; Tailor-Made Pore, J. D. Surface Engineering in Covalent Organic Frameworks: Systematic Functionalization for Performance Screening. *J. Am. Chem. Soc.* **2015**, *137*(22), 7079–7082. DOI: [10.1021/jacs.5b04300](https://doi.org/10.1021/jacs.5b04300).
- [5] Wasielewski, M. R. Photoinduced Electron Transfer in Supramolecular Systems for Artificial Photosynthesis. *Chem. Rev.* **1992**, *92*(3), 435–461. DOI: [10.1021/cr00011a005](https://doi.org/10.1021/cr00011a005).
- [6] Komatsu, T.; Moritake, M.; Molecular Energy, T. E. Electron Transfer Assemblies Made of Self-Organized Lipid-Porphyrin Bilayer Vesicles. *Chem. Eur. J.* **2003**, *9*(19), 4626–4633. DOI: [10.1002/chem.200305013](https://doi.org/10.1002/chem.200305013).
- [7] Velický, M.; Toth, P. S. From Two-Dimensional Materials to Their Heterostructures: An Electrochemist's Perspective. *Appl. Mater. Today.* **2017**, *8*, 68–103. DOI: [10.1016/j.apmt.2017.05.003](https://doi.org/10.1016/j.apmt.2017.05.003).
- [8] Moehwald, H.; Brezesinski, G. From Langmuir Monolayers to Multilayer Films. *Langmuir.* **2016**, *32*(41), 10445–10458. DOI: [10.1021/acs.langmuir.6b02518](https://doi.org/10.1021/acs.langmuir.6b02518).
- [9] Al-Alwani, A. J.; Shinkarenko, O. A.; Chumakov, A. S.; Pozharov, M. V.; Begletsova, N. N.; Kolesnikova, A. S.; Sevostyanova, V. P.; Glukhovskoy, E. G. Influence of Capping Ligands on the Assembly of Quantum Dots and Their Properties. *Mater. Sci. Technol.* **2019**, *35*(9), 1053–1060. DOI: [10.1080/02670836.2019.1612141](https://doi.org/10.1080/02670836.2019.1612141).
- [10] Shen, Y.; Zhan, F.; Lu, J.; Zhang, B.; Huang, D.; Xu, X.; Zhang, Y.; Wang, M. Preparation of Hybrid Films Containing Gold Nanoparticles and Cobalt Porphyrin with Flexible Electrochemical Properties. *Thin Solid Films.* **2013**, *545*, 327–331. DOI: [10.1016/j.tsf.2013.08.002](https://doi.org/10.1016/j.tsf.2013.08.002).
- [11] Johnson, R. W.; Hultqvist, A.; Bent, S. F.; Brief, A. Review of Atomic Layer Deposition: From Fundamentals to Applications. *Mater. Today.* **2014**, *17*(5), 236–246. DOI: [10.1016/j.mattod.2014.04.026](https://doi.org/10.1016/j.mattod.2014.04.026).
- [12] Helmersson, U.; Lattemann, M.; Bohlmark, J.; Ehasarian, A. P.; Gudmundsson, J. T. Ionized Physical Vapor Deposition (IPVD): A Review of Technology and Applications. *Thin Solid Films.* **2006**, *513*(1), 1–24. DOI: [10.1016/j.tsf.2006.03.033](https://doi.org/10.1016/j.tsf.2006.03.033).
- [13] Moreira, J.; Vale, A. C.; Alves, N. M. Spin-Coated Freestanding Films for Biomedical Applications. *J. Mater. Chem. B.* **2021**, *9*(18), 3778–3799. DOI: [10.1039/D1TB00233C](https://doi.org/10.1039/D1TB00233C).
- [14] Camacho, S. A.; Aoki, P. H. B.; Assis, F. F. D.; Pires, A. M.; Oliveira, K. T. D.; Constantino, C. J. L. Supramolecular Arrangements of an Organometallic Forming Nanostructured Films. *Mater. Res.* **2014**, *17*(6), 1375–1383. DOI: [10.1590/1516-1439.279014](https://doi.org/10.1590/1516-1439.279014).
- [15] Milyaeva, O. Y.; Akent'ev, A. V.; Bykov, A. G.; Zerov, A. V.; Isakov, N. A.; Noskov, B. A. Compression Isotherms of Polydopamine Films. *Colloid J.* **2020**, *82*(5), 546–554. DOI: [10.1134/S1061933X20050129](https://doi.org/10.1134/S1061933X20050129).
- [16] Li, S.; Micic, M.; Orbulescu, J.; Whyte, J. D.; Leblanc, R. M. Human Islet Amyloid Polypeptide at the Air-Aqueous Interface: A Langmuir Monolayer Approach. *J. R. Soc. Interface.* **2012**, *9*(76), 3118–3128. DOI: [10.1098/rsif.2012.0368](https://doi.org/10.1098/rsif.2012.0368).
- [17] Chumakov, A.; Al-Alwani, A. J.; Ermakov, A.; Shinkarenko, O.; Begletsova, N.; Glukhovskoy, E.; Santer, S. The Formation of Arachidic Acid Langmuir Monolayers on the NiCl₂ Solution. *J. Phys. Conf. Ser.* **2018**, *1124*, 081009. DOI: [10.1088/1742-6596/1124/8/081009](https://doi.org/10.1088/1742-6596/1124/8/081009).
- [18] Shinkarenko, O. A.; Chumakov, A. S.; Pozharov, M. V.; Kolesnikova, A. S.; Al-Alwani, A. J. K.; Tsvetkova, O. Y.; Sevostyanov, V. P.; Glukhovskoy, E. G. Study of the Possibility of Using Arachidic Acid as a Monocrystalline Substrate for the Formation of Monolayers of Aromatic Hydrocarbons. *J. Phys. Conf. Ser.* **2018**, *1124*, 081034. DOI: [10.1088/1742-6596/1124/8/081034](https://doi.org/10.1088/1742-6596/1124/8/081034).
- [19] Smirnova, A. I.; Soldatova, K. M.; Ezhov, A. V.; Bragina, N. A.; Giricheva, N. I.; Usol'tseva, N. V. Experimental and Theoretical Absorption Spectra of A3B-Type Porphyrine Derivatives. *Liq. Cryst. Appl.* **2019**, *19*(4), 25–37. DOI: [10.18083/LCAppl.2019.4.25](https://doi.org/10.18083/LCAppl.2019.4.25).
- [20] Казак, А. В.; Усольцева, Н. В.; Быкова, В. В.; Семейкин, А. С. Юдин, С. Г. Сравнительный анализ надмолекулярной организации в плавающих слоях мезо-замещенных тетрафенилпорфиринов. *Жидкие Кристаллы И Их Практическое Использование*, **2010**, No. 4 (34). (Kazak A.V.; Usol'tseva N.V.; Bykova V.V.; Semeikin A.S.; Yudin S.G. Comparative Analysis of Supramolecular Organization in Floating Layers of Meso-substituted Tetraphenylporphyrines. *Liq. Cryst. Appl.* **2010**, *4*(34), 90–97.
- [21] Gurkov, T. D.; Russev, S. C.; Danov, K. D.; Ivanov, I. B.; Campbell, B. Monolayers of Globular Proteins on the Air/Water Interface: Applicability of the Volmer Equation of State. *Langmuir.* **2003**, *19*(18), 7362–7369. DOI: [10.1021/la034250f](https://doi.org/10.1021/la034250f).
- [22] Caruso, B.; Ambroggio, E. E.; Wilke, N.; Fidelio, G. D. The Rheological Properties of Beta Amyloid Langmuir Monolayers: Comparative Studies with Melittin Peptide. *Colloids Surf. B Biointerfaces.* **2016**, *146*, 180–187. DOI: [10.1016/j.colsurfb.2016.06.003](https://doi.org/10.1016/j.colsurfb.2016.06.003).
- [23] Noskov, B. A.; Bykov, A. G. Dilational Surface Rheology of Polymer Solutions. *Russ. Chem. Rev.* **2015**, *84*(6), 634. DOI: [10.1070/RCR4518](https://doi.org/10.1070/RCR4518).
- [24] Wamke, A.; Dopierała, K.; Prochaska, K.; Maciejewski, H.; Biadasz, A.; Dudkowiak, A. Characterization of Langmuir Monolayer, Langmuir–Blodgett and Langmuir–Schaefer

- Films Formed by POSS Compounds. *Colloids Surf. Physicochem. Eng. Asp.* **2015**, 464, 110–120. DOI: [10.1016/j.colsurfa.2014.10.022](https://doi.org/10.1016/j.colsurfa.2014.10.022).
- [25] Nath, J.; Nath, R. K.; Chakraborty, A.; Husain, S. A. Monolayer Characteristics of Chitosan Assembled in Langmuir Films Mixed with Arachidic Acid. *Surf. Rev. Lett.* **2014**, 21(4), 1450049. DOI: [10.1142/S0218625X14500498](https://doi.org/10.1142/S0218625X14500498).
- [26] Xu, G.; Hao, C.; Zhang, L.; Sun, R. Investigation of Surface Behavior of DPPC and Curcumin in Langmuir Monolayers at the Air-Water Interface. *Scanning.* **2017**, 2017, 6582019. DOI: [10.1155/2017/6582019](https://doi.org/10.1155/2017/6582019).
- [27] Al-Alwani, A. J.; Chumakov, A.; Shinkarenko, O.; Qassime, M.; Begletsova, N.; Gorbachev, I.; Venig, S.; Kazak, A.; Glukhovskoy, E. Effect of Subphase Conditions on the Formation of Graphene Langmuir Layers. *J. Phys. Conf. Ser.* **2018**, 1135, 012029. DOI: [10.1088/1742-6596/1135/1/012029](https://doi.org/10.1088/1742-6596/1135/1/012029).
- [28] Modlińska, A.; The Langmuir-Blodgett, B. D. Technique as a Tool for Homeotropic Alignment of Fluorinated Liquid Crystals Mixed with Arachidic Acid. *Int. J. Mol. Sci.* **2011**, 12(8), 4923–4945. DOI: [10.3390/ijms12084923](https://doi.org/10.3390/ijms12084923).
- [29] Dynarowicz-Łątka, P.; Kita, K. Molecular Interaction in Mixed Monolayers at the Air/Water Interface. *Adv. Colloid Interface Sci.* **1999**, 79(1), 1–17. DOI: [10.1016/S0001-8686\(98\)00064-5](https://doi.org/10.1016/S0001-8686(98)00064-5).
- [30] Bykov, A. G.; Guzmán, E.; Rubio, R. G.; Krycki, M. M.; Milyaeva, O. Y.; Noskov, B. A. Influence of Temperature on Dynamic Surface Properties of Spread DPPC Monolayers in a Broad Range of Surface Pressures. *Chem. Phys. Lipids.* **2019**, 225, 104812. DOI: [10.1016/j.chemphyslip.2019.104812](https://doi.org/10.1016/j.chemphyslip.2019.104812).
- [31] Nguyen, L.-T.-T.; Ardana, A.; Ten Brinke, G.; Schouten, A. J. Surface Potentials in Langmuir Monolayers of Unidirectionally Oriented α -Helical Diblock Copolypeptides. *Langmuir.* **2010**, 26(9), 6515–6521. DOI: [10.1021/la904007m](https://doi.org/10.1021/la904007m).
- [32] Ku, T.; Gill, S.; Löbenberg, R.; Azarmi, S.; Roa, W.; Prenner, E. J. Size Dependent Interactions of Nanoparticles with Lung Surfactant Model Systems and the Significant Impact on Surface Potential. *J. Nanosci. Nanotechnol.* **2008**, 8(6), 2971–2978. DOI: [10.1166/jnn.2008.171](https://doi.org/10.1166/jnn.2008.171).